IEEE Access
Multidisciplinary | Rapid Review | Open Access Journal

Received 6 December 2023, accepted 2 January 2024, date of publication 5 January 2024, date of current version 24 January 2024.

Digital Object Identifier 10.1109/ACCESS.2024.3350270

RESEARCH ARTICLE

Mid-Infrared Hollow-Core Waveguide Gas Sensor for Low-Concentration Sulfur Hexafluor Detection

FENG ZHOU, (Senior Member, IEEE), JICHENG YU, (Senior Member, IEEE), XIAODONG YIN, CHANGXI YUE, AND SIYUAN LIANG

China Electric Power Research Institute, Wuhan 430074, China

Corresponding author: Jicheng Yu (yujicheng@epri.sgcc.com.cn)

This work was supported by the State Grid Corporation of China Science and Technology Project under Grant 5400-202255274A-2-0-XG.

ABSTRACT Sulfur hexafluoride gas (SF_6) is widely used in various electrical insulating equipment in the electric power industry. In this paper, a novel mid-infrared hollow-core fiber (HCF) gas sensor based on infrared spectral absorption is proposed for low-concentration SF_6 leakage detection. The fiber was coupled with the mid-infrared source and detector directly through a mechanical process interface. With a narrow filter, target gas absorption band light was filtered out. The optimal length of the optical fiber is derived by theoretical modeling and optimization solutions. The experimental results show that the sensor has sub-ppm measurement limitation for SF_6 gas by utilizing a Lab-view-based digital dual-phase lock-in amplifier. The calibration results of SF_6 standard gas at concentrations of 0.5 ppm, 2.45 ppm, 4.9 ppm, and 9.92 ppm show that the detection error of the sensor is less than 1%. Repeatability test results show the sensor can achieve high stability and low zero drift. It provides a compact and low-cost solution for low-concentration SF_6 detection in the environment.

INDEX TERMS Hollow-core waveguide, infrared adsorption spectrum, SF_6 sensor.

I. INTRODUCTION

Sulfur hexafluoride gas (SF_6) is widely used in various electrical insulating equipment in the electric power industry due to its high stability, strong electrical insulation strength, and excellent arc extinguishing ability. However, due to its gas dispersion behavior, the leakage is prone to occur during such as production, processing, equipment installation, and maintenance. It will cause various extent damage to the performance of the electrical equipment, the safety of the operators, and especially the atmospheric environment, etc. With the rapid development of gas-insulated electrical equipment, the complexity of electric power in transmission, transformation, and distribution processes puts forward a new demand for online real-time monitoring of the leakage of SF_6 gas.

As reported, SF_6 gas detection methods mainly include photoacoustic spectroscopy technology [1], infrared imaging technology [2], ion mobility spectrometry [3], and non-dispersive IR (NDIR) [4]. With the advancement of medium-infrared fiber, the hollow-core optical fiber (HCF), which uses its inner cavity as a gas absorption cell, can realize the simultaneous transmission of gas molecules and their absorption band signals. This performance helps simplify optical path design, improve the light and gas interaction distance, enhance detection accuracy, et al. With the development and maturity of micromachining and optical integration technology, the integration of HCF and various optical devices with higher sensitivity in a smaller volume shows great potential in environmental gas monitoring [5], [6].

The HCFs currently used for gas detection include hollow-core photonic crystal fiber [7], [8], anti-resonant HCF [9], and hollow-core waveguide fiber [10]. In the near-infrared band, a variety of HCFs have been studied for gas monitoring applications [11]. Harrington et al. carried out research on the fabrication process of special HCW with AgI inner coating in the 1990s and used it as absorption cells to construct VOC gas detection devices based on the non-dispersive infrared principle [12]. Chen et al. designed an all-fiber ethane gas sensor by using a single-mode fiber collimated with an HCF, which achieved a detection limit of 13 ppb and had the advantages of stability and compactness, but the single-mode

The associate editor coordinating the review of this manuscript and approving it for publication was Sukhdev Roy.

fiber had a large light intensity loss at the docking place of the single-mode fiber and the HCF, and the coupling efficiency was low [13]. In the same year, Jaworski et al. proposed a methane and carbon dioxide dual-gas detection sensor based on wavelength modulation spectroscopy, which realized a detection limit of 24 ppb for methane and 144 ppm for carbon dioxide [14]. However, the sensor requires multiple lenses and other coupling devices, which makes the structural design more complicated and requires three lasers, which greatly increases the cost. The team of Jin Wei from the University of Hong Kong used a 13 m long hollow-core photonic bandgap optical fiber to reduce the modal interference and achieved a detection limit of 1 ppm for acetylene gas, but the excessively long optical fiber greatly increased the response time and cost of the sensor [15]. By 2020, the team used wavelength modulation spectroscopy to design a nitric oxide gas detection sensor, and by designing free-space coupling optics, the coupling efficiency reached 90%, with a detection limit of 13 ppm [16]. However, the system also used more collimating lenses and parabolic mirrors, and the structural design was more complex, which was not conducive to the integration. To improve the sensor performance, Arman et al. studied the gas sensitive model and proposed an optimization method for the photonic crystal HCF sensor [17], [18]. It has been proved that the confinement loss and sensitivity can be improved through mode interference elimination and size optimization of the fiber. Currently, the commonly used gas injection method is to fill the end face of the HCF [19], which means the air inlet and outlet sealing device and the optical coupling device overlap. Piotr Jaworski et al. have found that the gas filling time of hollow core optical fibers decreases with the increase of the inner diameter size of the hollow core [20]. Therefore, the gas filling time can be shortened by choosing hollow core waveguide fiber, which has an inner cavity of several hundred microns, which is much larger than that of hollow photonic crystal fiber and anti-resonant HCF. Studies have shown that the HCF loss increases with the wavelength of the transmitted optical signal [21], the current HCF gas detection technology has not yet matured, and the cost of the corresponding optical coupling device is high.

The SF_6 strong absorption peak is around the 10.55 μm band, which can be covered by CO_2 laser, Quantum Cascade laser(QCL), and the traditional blackbody radiation source. M. Rocha et al. have reported two photoacoustic spectroscopy based SF_6 sensors and compared the CO_2 laser and QCL [22]. The results show that the CO_2 laser with a higher optical intensity of 1.9 W can effectively increase the detection limit from 50 ppb to 20 ppb compared to the QCL which is only 3.7 mW. J. S. Li et al. reviewed the trend of quantum lasers in Atmospheric Chemistry, which can cover more than ten gases including SF_6 in the mid-infrared region, as compared to the CO_2 laser with a single output wavelength [23]. The QCL can cover the mid-infrared region from 3.5 to 24 μm, covering more than ten gas absorption wavelengths including SF_6. Moreover, the QCL wavelength can be tuned within a certain range, which can greatly simplify the light source components when constructing a multi-gas detection system. Xingyu Pan et al. have constructed an SF_6 monitoring system by using a tunable outer-cavity interferometric QCL light source in the range of 6.7 μm to 8.7 μm and a miniaturized quartz crystal tuning fork [24]. Based on this light source, the system obtained a detection limit of 1.89 ppm and good linearity in the SF_6 absorption region in the 7.12 to 7.96 μm band. Sherstov et al. have used a CO_2 laser to improve the measurement limit of an SF_6 monitoring device to 0.1 ppb by optimizing the design of an optoacoustic cell, while the system can cover 100% concentration of SF_6 monitoring across multiple orders of magnitude, with an overall measurement error of less than 10% [25]. Despite the advantages, the miniaturization of CO_2 laser tubes is still difficult and makes it a problem to improve the integration of the device. Moreover, QCL has a weakness of high cost, which makes it limited to the analysis in the laboratory application. Traditional infrared light sources can meet the requirements of miniaturization and low cost. Dong et al. have used an infrared broad-spectrum light source design for the SF_6 decomposition gas monitoring system [26]. However, the infrared light source for SF_6 itself in the 10.55 μm absorption band is still weak and difficult to couple with.

In this paper, we proposed a novel design of an SF_6 sensor with a hollow-core optical waveguide directly coupled to an infrared blackbody light source. By utilizing an ultra-narrow band mid-infrared filter, the light aimed at the SF_6 absorbing band around 10.55 μm was acquired. The optimal length of the optical fiber is derived by theoretical modeling and optimization solutions. Through a mechanical processed optical and pneumatic coupling interface, the platform has been built. Based on a digital dual phase lock-in amplifier, the weak gas absorption light intensity change signal is analyzed and identified. It provides an effective solution for highly sensitive and low-cost SF_6 gas monitoring. Moreover, it has the potential to be applied to multi-gas monitoring by utilizing various optical filters.

II. SF_6 DETECTION PRINCIPLE

A. GAS CONCENTRATION CALCULATION MODEL

The SF_6 concentration detection by NDIR method is based on the Lambert-Beer law. After passing through gas molecules with a specific absorption peak, the light intensity of the corresponding wavelength will be attenuated. The amplitude of the attenuation is related to the absorption coefficient of the gas molecule, the optical range length, and the gas concentration as the following equation:

$$I_o = I_i e^{-\alpha c l} \tag{1}$$

where I_i and I_o are the input and output light intensity respectively; α is the absorption coefficient of the gas molecule to be measured (cm^{-1}); C is the concentration of the gas to be measured; l is the optical range length (cm). From the formula, when the gas absorption coefficient and the optical range length are determined, the concentration of the gas to

be measured can be calculated by the change of light intensity before and after the gas chamber.

From (1), the concentration of the gas to be measured is:

$$C = -\frac{1}{\alpha l} \ln \frac{I_o}{I_i} \tag{2}$$

Considering the test system accomplishes photoelectric conversion at a constant factor, it is common to use the voltage V to replace the light intensity I. The relational equation between them can be converted as follows:

$$\frac{V\prime}{V_0} = \frac{I_o}{I_i} = e^{-\alpha c l} \tag{3}$$

where V_0 is the initial voltage value and $V\prime$is the voltage value when the target gas is filled. Hence, the concentration of the gas can be expressed as:

$$C = -\frac{1}{\alpha l} \ln \frac{V\prime}{V_0} \tag{4}$$

B. MODEL ANALYSIS OF OPTIMAL FIBER COUPLING LENGTH

The absorption spectra of gas molecules for gas sensors based on the NDIR method are shown in Fig. 1. From Fig.1 (a), the absorption peak of SF_6 is located around 10.55 μm, which is not overlapped with other common environmental gases, and its decomposed gas molecules [26]. Hence, the intensity of the absorbed light signal of SF_6 at 10.6 μm is not disturbed by other absorbing molecules in the detection process. The absorption spectrum of SF_6 in the mid-infrared region can be obtained from the HITRAN database, as shown in Fig. 1(b). It depicts the absorption intensity of SF_6 gas in the 930-960 cm^{-1} waveband range at 101 kPa and room temperature of 20°C. As shown in Fig. 1, the SF_6 has the strongest absorption coefficient at the wave number of 947.93 cm^{-1}, which is about 7.48 $\times$ 10^{-4} cm^{-1}, corresponding to the wavelength of 10.55 μm. Since the broadband optical signal is filtered by a narrow-band filter after gas absorption, there is no other gas absorption within the bandwidth of the filter, so it will not affect the measurement results.

Set the length of the optical fiber to be $L$and the loss coefficient to be α_f (dB/m). When there is no gas filled into the core area of the HCF, only the transmission loss of the fiber is considered. The optical loss of the HCF, in dB units, can be expressed from the light intensity ratio of the input I_i and the output I_o as follows:

$$\alpha_f L = 10 \lg \frac{I_i}{I_o} \tag{5}$$

Hence, the output I_o can be expressed as,

$$I_o = I_i 10^{-\frac{\alpha_f}{10} L} \tag{6}$$

When the target gas is filled in the fiber with a concentration of C, considering transmission loss including HCF itself and the gas absorption, the output light intensity changes to $I_o\prime$ according to equations (1) and (6) as follows:

$$I_o\prime = I_i 10^{-\frac{\alpha_f}{10} L} e^{-\alpha_g C L} \tag{7}$$

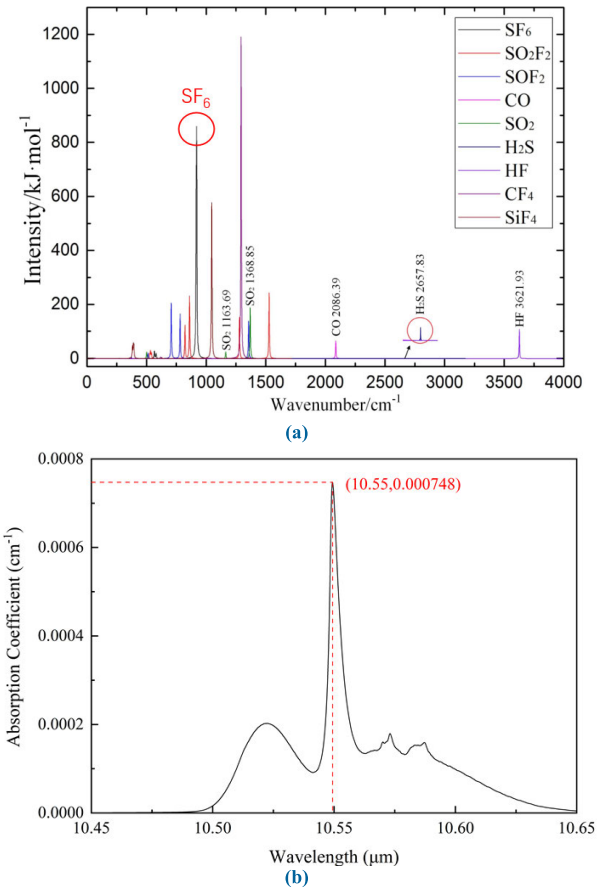

FIGURE 1. Absorption spectra of gas molecules for NDIR method. (a) Comparison of different gas absorption spectra [23]; (b)SF_6 gas absorption spectra from the HITRAN database.

where the absorption coefficient of the gas at a certain wavelength is α_g.

Set the minimum change in light intensity that can be resolved by the detector to be $\Delta I_{min} = I_i - I_O'$, then the gas concentration detection limit $C_{\min}$ of the system can be derived from (6) as:

$$C_{\min} = \frac{-\ln(1 - \frac{\Delta I_{\min}}{I_i} 10^{\frac{\alpha_f}{10} L})}{\alpha_g L} \tag{8}$$

Since $I_i \gg \Delta I_{\min}$, a 1st-order Taylor expansion can be taken for the numerator in (8), which simplifies to:

$$C_{\min} = \frac{\Delta I_{\min}}{I_i} \frac{1}{\alpha_g L} 10^{\frac{\alpha_f}{10} L} \tag{9}$$

where the parameters $\Delta I_{\min}$ and I_i are constants that depend on the light source and detector in a certain system. As the following formula, the minimum point of $C_{\min}$ can be obtained by solving the equation that makes the partial derivative of $C_{\min}$ to L zero.

$$\frac{dC_{\min}}{dL} = \frac{\Delta I_{\min}}{I_i \alpha_g} \frac{\frac{\alpha_f \ln 10}{10} 10^{\frac{\alpha_f}{10} L} L - 10^{\frac{\alpha_f}{10} L}}{L^2} \tag{10}$$

TABLE 1. Parameters of the HCF.

Type	HWG 500
Inner Diameter, μm	500
Outer Diameter, μm	650
Attenuation Coefficient at 10.6μm Waveleng, dB/m	0.7
Bending Loss Coefficient in Radius of 100 mm, dB/m	1.5
Length, m	2
Type of Fiber Connector	SMA905

The optimal fiber length L_{op} can be obtained as:

$$L_{op} = \frac{10}{\ln 10}\frac{1}{\alpha_f} \tag{11}$$

III. EXPERIMENTAL SETUP

A. STRUCTURE OF THE SF_6 GAS SENSOR

The schematic diagram of the SF_6 gas sensor based on HCF is shown in Fig. 2. The HCF (HWG 500, Art Photonics Company) is armored with a jacket and packaged in SMA905 connectors for its two ends. The parameters of HWG are shown in Table 1. It was directly coupled with the infrared blackbody light source and infrared detector through the mechanically processed SMA fiber holder with a bending radius of 100 mm. According to Table 1, the bending loss coefficient of the HCF is 1.5 dB/m from the product report that tested with 2 m length and 200 mm diameter HCF. Substituting into equation (11), the optimal length of the optical fiber is 2.89 m, which is rounded down to 2 m limited by available commercial product specifications.

The gas sensor is powered by a switching power supply, while the internal components including the light source, detector, and amplifier are powered by a voltage regulator module. The infrared blackbody light source (JSIR 350-4, Micro-Hybrid) has an output wavelength range of 2-15 μm, 130 mW output intensity in total, and 0.1 mW in the SF_6 target band. The detector (PVMI-4TE-10.6, VIGO) has a detection range of 2-15 μm and a detectivity of 2.5×10^9 cm·Hz$^{1/2}$/W at 10.6 μm. A WIFI wireless I/O module that provides a Labview program interface processes the modulation and demodulation functions of the weak light signal. The 5 Hz PWM voltage output is used to drive and modulate the light source signal, while 24-bit 0-10 V high-precision voltage acquisition (Vk701-w, Vking) is utilized to acquire the detector's photoelectric conversion voltage.

As shown in Fig. 3, the optical coupling structure mainly includes the HCF-detector coupling structure and the HCF-light source coupling structure, which are connected by the HCF through the standard SMA905 ports. Through this structure, the broadband light signal from the light source can be coupled into the HCF and absorbed by SF_6 test gas, and then transmitted through the narrow-band filter and received by the optical probe of the detector.

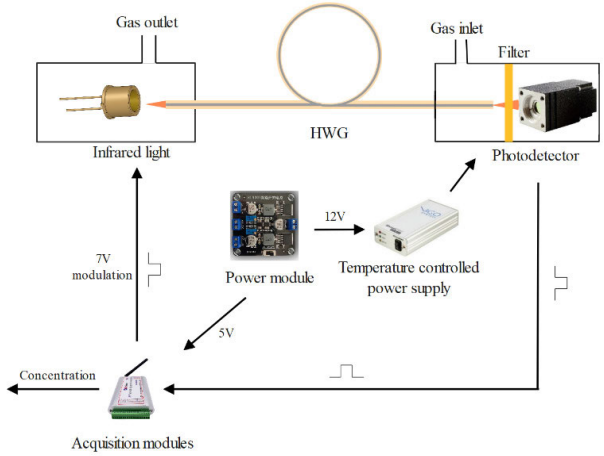

FIGURE 2. Schematic diagram of gas detection sensor.

The schematic diagram of the HCF-detector coupling structure is shown in Fig. 3(a). It consists of a detector, filter, adapter, SMA socket, and tee connector. One side of the HCF is fixed on the adapter through the SMA Socket, on which there are two gas holes punched. The other side passes through the horizontal channel of a tee connector and connects to one end of it by a seal cap. Between the adapt and the detector base, there is a narrow band 10.6 μm filter with a half-peak width of 240 nm, which is sealed in the middle like a sandwich structure by a sealing gasket. The test gas can enter the adapter through the vertical hole of the tee connector and pass through the via holes in the socket to fill into one end of the HCF. The blue arrow in the figure indicates the direction of gas flow.

The HCF-light source coupling structure consists of an optical adapter, infrared light source, lens tube, and SMA socket, as shown in Fig. 3(b). One side of the HCF that passes through the tee connector is connected to the SMA socket, which is fixed with the adapter through the lens tube. The light source can be efficiently coupled to the HCF by using the pitch angle adjustment feature of the adapter. The gas flow from the HCF is directly discharged through gaps between the light source, fiber, and adapter.

As shown in Fig. 4, the circuit part and the detection probe are integrated into a compact case. The light source coupling structure and detector coupling structure are fixed in the chassis. The hollow core optical fiber is coiled in the 3D printed bracket with a radius of 100 mm to make it resistant to environmental vibration. The pneumatic three-way valve was connected to the two, in which the optical fiber and the detector connected to the end of the set of a section of sealant tube. The detection system through the pneumatic three-way valve into the air and fills the sealing tube gas chamber, and then through the HCF end face into the hollow cavity and infrared light absorption reaction.

To demodulate modulated optical signals from noise and make the detection results more stable, the lock-in amplification module was constructed in the upper computer program using Labview programming, which makes the voltage

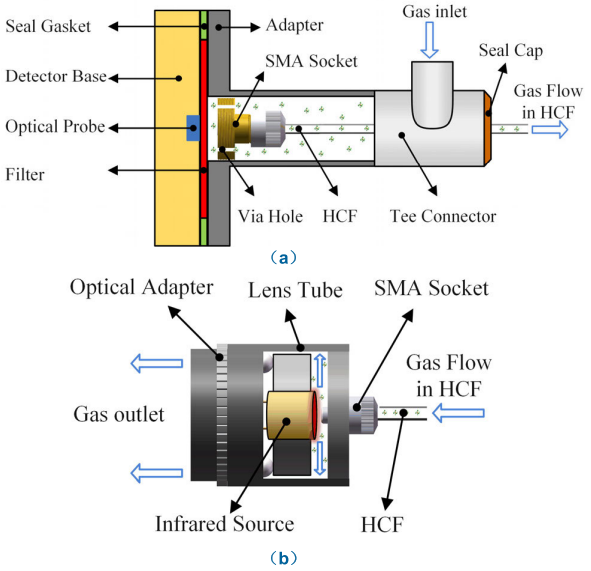

FIGURE 3. Schematic diagram of sensor optical path coupling structure. (a) HCF-detector coupling structure; (b) HCF-light source coupling structure.

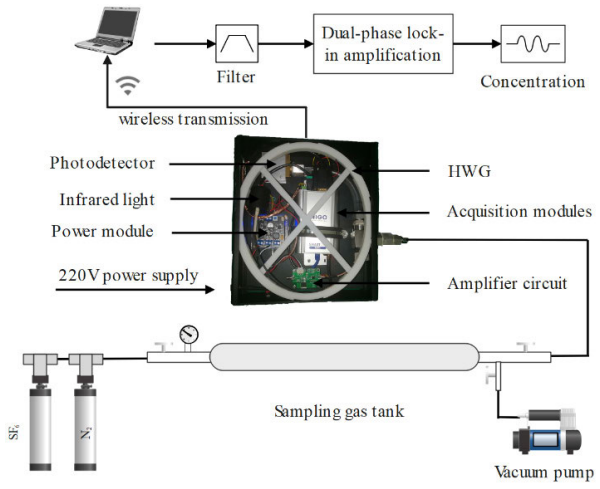

FIGURE 4. Schematic diagram of gas test system.

fluctuations less than 1 μV. In addition, it is a dual-phase lock-in structure to eliminate the changes in signal strength caused by the phase fluctuation of the digital PWM signal.

IV. RESULTS AND DISCUSSION

The gas response of this sensor was tested on the built gas test system. According to Equation (4), the initial voltage value of the sensor V_0 was measured first. Then, various concentrations of SF_6 and N_2 mixed standard gas were filled into the three-way valve to carry out gas concentration calibration experiments. The gas will absorb part of the infrared light intensity around the 10.55μm band which goes through the HCF. Then, the voltage value after gas absorption $V\prime$ was measured.

As shown in Fig. 5, the voltage value remained at 71 μV in the initial state and started to decrease after the SF_6 gas was filled. The response amplitude decreased with the increase of

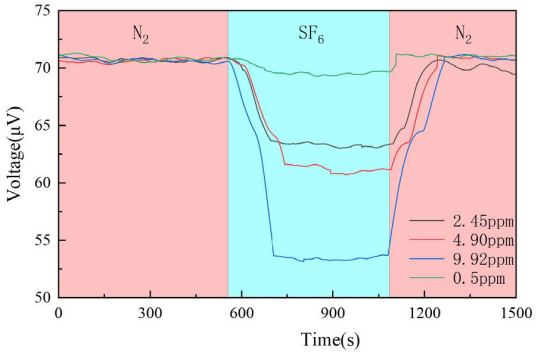

FIGURE 5. Voltage change curve of the sensor after gas absorption.

gas concentration. The response and recovery speed of the gas is determined by the flow rate of the input gas, which was controlled through a mass flow controller at 5 sccm to maintain laminar flow and low pressure loss in HCF. For the 2 m length HCF, the response and recovery time was around 150 s.

The response time here consists of two parts, one is the filling time of the gas in the HCF and the other is the mixing time of the gas in the Fiber-light source coupling structure. As the volume of the inner cavity of the hollow fiber is about 1.5 cm^3, the gas filling time is approximately 4.7 s under the flow rate of 5 sccm ideally. However, before entering the HCF, the gas flow needs to pass through the sampling gas tank, pipeline, and the Fiber-light source coupling structure. Although the vacuum pump can remove most part residual SF_6 and N_2 gas from the test system, it still needs a long gas mixing and diffusion process to make the concentration of the test gas get a steady state, especially for the target SF_6 gas at ppm level. Hence, the response time is much longer than the gas filling time in the HCF under ideal calculation.

In order to verify the repeatability of the sensor, each component of the standard mixture of gases was measured two times. The results of the experiment are shown in Fig. 6. The amplitude of the sensor at zero and response points over many repetitions are stable with a fluctuation range of less than 1 μV.

In the process of filling test gas, the transmitted light intensity in the sensor is reduced due to gas absorption, while inducing the drops of detector voltage. At the end of the response, nitrogen is injected and the detector voltage returns to the zero reference value. The amplitude of the sensor at zero and response points over many repetitions are stable with a fluctuation range of less than 1 μV. Measurements at different concentrations show that the sensor is sensitive in the range of 0.5 ppm to 10 ppm. Furthermore, a good amplitude consistency is shown during repeated tests. The zero point value that fluctuates after 8 cycles is about 0.45 μV, which is about 0.6% to the initial voltage of 71.17 μV.

The sensitivity calibration of gas concentration is carried out by the voltage data of the detected signal before and after the absorption of SF_6. From (4), the gas absorption curve was fitted according to the experimental data, which is shown in

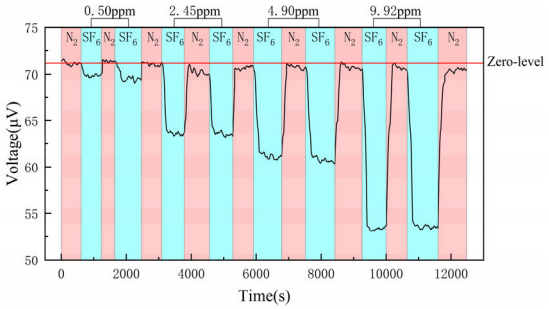

FIGURE 6. Multi-cycle response experiments with different concentrations of SF_6 gas.

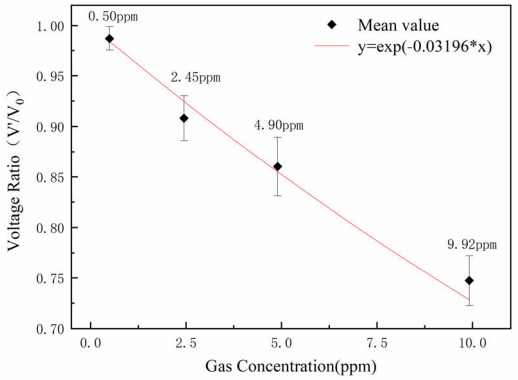

FIGURE 7. Gas absorption response fitting curve.

TABLE 2. Comparison of different SF_6 gas sensors.

Literature	Working Principle	Detection Limit
This paper	Non-dispersive IR	0.5 ppm
Sampaolo, A et al. [1]	Photoacoustic spectrometry	2.7 ppb
Lu, Q. et al. [2]	Infrared imagery	0.06 ml/min
W. Huang et al. [3]	Ion mobility spectrometry	0.16-0.68 ppm
Li, J. et al. [4]	Non-dispersive IR	0.01%

Fig. 7. The fitting expression is as follows:

$$y = e^{-0.3031x} \tag{12}$$

where y is the ratio of voltage before and after gas absorption and x is the gas concentration. The fitting correlation coefficient R^2 is 0.986.

Based on the fitting results, the maximum deviation in the response of this sensor occurs at the 2.45 ppm gas measurement point. However, the deviation value does not exceed 1%, which indicates that the sensor has a high measurement accuracy.

As shown in TABLE 2, the SF_6 sensor proposed in this paper has a lower detection limit compared to most other methods. Due to the use of mid-infrared HCF as the gas absorber cell, facing the different requirements for the different detection applications, it is flexible to adjust the length of the HCF to increase or reduce the resolution. It represents a promising application of the sensor in low-concentration SF_6 leakage monitoring.

V. CONCLUSION

In this paper, a novel mid-infrared HCF SF_6 gas sensor based on infrared spectral absorption is proposed. The simplified design of the optical path through a direct-coupled structure allows the sensor to have a compact size and low cost. The SF_6 gas with a concentration of sub-ppm can be detected by utilizing a Labview-based digital dual-phase lock-in amplifier. The calibration results of SF_6 standard gas at concentrations of 0.5 ppm, 2.45 ppm, 4.9 ppm, and 9.92 ppm show that the detection error of the sensor is less than 1%. Repeatability test results show the sensor can achieve high stability and low zero drift.

ACKNOWLEDGMENT

The authors are deeply grateful to an Associate Prof. Song Han and his Group, School of Electrical and Mechanical Engineering, Wuhan University of Technology, for providing the test equipment and SF_6 calibrating gas.

REFERENCES

[1] A. Sampaolo, P. Patimisco, M. Giglio, L. Chieco, G. Scamarcio, F. K. Tittel, and V. Spagnolo, "Highly sensitive gas leak detector based on a quartz-enhanced photoacoustic SF_6 sensor," *Opt. Exp.*, vol. 24, no. 14, pp. 15872–15881, Jul. 2016, doi: 10.1364/OE.24.015872.

[2] Q. Lu, Q. Li, L. Hu, and L. Huang, "An effective low-contrast SF_6 gas leakage detection method for infrared imaging," *IEEE Trans. Instrum. Meas.*, vol. 70, pp. 1–9, Apr. 2021, doi: 10.1109/TIM.2021.3073443.

[3] W. Huang, W. Wang, C. Chen, Y. Li, Z. Wang, Q. Li, M. Li, and K. Hou, "Real-time monitoring traces of SF_6 in near-source ambient air by ion mobility spectrometry," *Int. J. Environ. Anal. Chem.*, vol. 99, no. 9, pp. 868–877, Jul. 2019, doi: 10.1080/03067319.2019.1616709.

[4] W. Qing, L. Wei-long, and L. Yong-ping, "Design of non-dispersive infrared (NDIR) SF_6 gas monitoring system based on RBF neural network," in *Proc. Power Syst. Green Energy Conf. (PSGEC)*, Aug. 2022, pp. 965–968, doi: 10.1109/PSGEC54663.2022.9881186.

[5] S.-S. Kim, C. Young, and B. Mizaikoff, "Miniaturized mid-infrared sensor technologies," *Anal. Bioanal. Chem.*, vol. 390, no. 1, pp. 231–237, Jan. 2008, doi: 10.1007/s00216-007-1673-5.

[6] J. J. R. Rohwedder, C. Pasquini, P. R. Fortes, I. M. Raimundo, A. Wilk, and B. Mizaikoff, "IHWG-μNIR: A miniaturised near-infrared gas sensor based on substrate-integrated hollow waveguides coupled to a micro-NIR-spectrophotometer," *Analyst*, vol. 139, no. 14, pp. 3572–3576, Mar. 2014, doi: 10.1039/c4an00556b.

[7] N. Li, L. Tao, H. Yi, C. S. Kim, M. Kim, C. L. Canedy, C. D. Merritt, W. W. Bewley, I. Vurgaftman, J. R. Meyer, and M. A. Zondlo, "Methane detection using an interband-cascade LED coupled to a hollow-core fiber," *Opt. Exp.*, vol. 29, no. 5, pp. 7221–7231, Mar. 2021, doi: 10.1364/OE.415724.

[8] G. Gomólka, D. Pysz, R. Buczynski, and M. Nikodem, "Dual-pass hollow-core fiber gas spectroscopy using a reflective configuration with heterodyne-based signal detection," *J. Lightw. Technol.*, vol. 41, no. 18, pp. 6094–6101, Mar. 2023, doi: 10.1109/JLT.2023.3272308.

[9] R. Yu, Y. Chen, L. Shui, and L. Xiao, "Hollow-core photonic crystal fiber gas sensing," *Sensors*, vol. 20, no. 10, p. 2996, May 2020, doi: 10.3390/s20102996.

[10] C. Young, S. Hartwig, A. Lambrecht, S. S. Kim, and B. Mizaikoff, "Optimizing gas sensors based on quantum cascade lasers and photonic bandgap hollow waveguides," in *Proc. SENSORS*, Oct. 2007, pp. 1345–1348, doi: 10.1109/ICSENS.2007.4388660.

[11] J. Li, H. Yan, H. Dang, and F. Meng, "Structure design and application of hollow core microstructured optical fiber gas sensor: A review," *Opt. Laser Technol.*, vol. 135, Mar. 2021, Art. no. 106658, doi: 10.1016/j.optlastec.2020.106658.

[12] D. J. Haan and J. A. Harrington, "Hollow waveguides for gas sensing and near-IR applications," *Proc. SPIE*, vol. 3596, pp. 43–49, Apr. 1999, doi: 10.1117/12.346725.

[13] F. Chen, S. Jiang, W. Jin, H. Bao, H. L. Ho, C. Wang, and S. Gao, "Ethane detection with mid-infrared hollow-core fiber photothermal spectroscopy," *Opt. Exp.*, vol. 28, no. 25, pp. 38115–38126, Dec. 2020, doi: 10.1364/OE.410927.
[14] P. Jaworski, P. Kozioł, K. Krzempek, D. Wu, F. Yu, P. Bojęś, G. Dudzik, M. Liao, K. Abramski, and J. Knight, "Antiresonant hollow-core fiber-based dual gas sensor for detection of methane and carbon dioxide in the near- and mid-infrared regions," *Sensors*, vol. 20, no. 14, p. 3813, Jul. 2020, doi: 10.3390/s20143813.
[15] C. Yao, L. Xiao, S. Gao, Y. Wang, P. Wang, R. Kan, W. Jin, and W. Ren, "Sub-ppm CO detection in a sub-meter-long hollow-core negative curvature fiber using absorption spectroscopy at 2.3 μm," *Sens. Actuators B, Chem.*, vol. 303, Jan. 2020, Art. no. 127238, doi: 10.1016/j.snb.2019.127238.
[16] F. Yang, W. Jin, Y. Cao, H. L. Ho, and Y. Wang, "Towards high sensitivity gas detection with hollow-core photonic bandgap fibers," *Opt. Exp.*, vol. 22, no. 20, pp. 24894–24907, Oct. 2014, doi: 10.1364/OE.22.024894.
[17] H. Arman and S. Olyaee, "Improving the sensitivity of the HC-PBF based gas sensor by optimization of core size and mode interference suppression," *Opt. Quantum Electron.*, vol. 52, no. 9, pp. 1–10, Sep. 2020, doi: 10.1007/s11082-020-02538-8.
[18] H. Arman and S. Olyaee, "Realization of low confinement loss acetylene gas sensor by using hollow-core photonic bandgap fiber," *Opt. Quantum Electron.*, vol. 53, no. 6, p. 328, Jun. 2021, doi: 10.1007/s11082-021-02969-x.
[19] L. Liu, B. Xiong, Y. Yan, J. Li, and Z. Du, "Hollow waveguide-enhanced mid-infrared sensor for real-time exhaled methane detection," *IEEE Photon. Technol. Lett.*, vol. 28, no. 15, pp. 1613–1616, Aug. 2016, doi: 10.1109/LPT.2016.2559528.
[20] P. Jaworski, K. Krzempek, G. Dudzik, P. J. Sazio, and W. Belardi, "Nitrous oxide detection at 5.26 μm with a compound glass antiresonant hollow-core optical fiber," *Opt. Lett.*, vol. 45, no. 6, pp. 1326–1329, Mar. 2020, doi: 10.1364/OL.383861.
[21] F. Yu, P. Song, D. Wu, T. Birks, D. Bird, and J. Knight, "Attenuation limit of silica-based hollow-core fiber at mid-IR wavelengths," *APL Photon.*, vol. 4, no. 8, Aug. 2019, Art. no. 080803, doi: 10.1063/1.5115328.
[22] M. Rocha, M. Sthel, G. Lima, M. D. Silva, D. Schramm, A. Miklós, and H. Vargas, "A sulfur hexafluoride sensor using quantum cascade and CO_2 laser-based photoacoustic spectroscopy," *Sensors*, vol. 10, no. 10, pp. 9359–9368, Oct. 2010, doi: 10.3390/s101009359.
[23] J. S. Li, W. Chen, and H. Fischer, "Quantum cascade laser spectrometry techniques: A new trend in atmospheric chemistry," *Appl. Spectrosc. Rev.*, vol. 48, no. 7, pp. 523–559, Oct. 2013, doi: 10.1080/05704928.2012.757232.
[24] X. Pan, Y. Zhang, J. Zeng, M. Zhang, and J. Li, "External-cavity quantum cascade laser-based gas sensor for sulfur hexafluoride detection," *Chemosensors*, vol. 11, no. 1, p. 30, Dec. 2022, doi: 10.3390/chemosensors11010030.
[25] I. V. Sherstov and V. A. Vasiliev, "Highly sensitive laser photo-acoustic SF_6 gas analyzer with 10 decades dynamic range of concentration measurement," *Infr. Phys. Technol.*, vol. 119, Dec. 2021, Art. no. 103922, doi: 10.1016/j.infrared.2021.103922.
[26] M. Dong, C. Zhang, M. Ren, R. Albarracín, and R. Ye, "Electrochemical and infrared absorption spectroscopy detection of SF_6 decomposition products," *Sensors*, vol. 17, no. 11, p. 2627, Nov. 2017, doi: 10.3390/s17112627.

FENG ZHOU (Senior Member, IEEE) received the bachelor's and master's degrees in automation from the Hefei University of Technology, Hefei, China, and the Ph.D. degree in high-voltage and insulation from the Huazhong University of Science and Technology, Wuhan, China.

Currently, he is the Director of the Institute of Metrology, China Electric Power Research Institute. He has authored five books, more than 50 articles, and more than 80 inventions. His research interests include high-voltage insulation and high-voltage and high-current measurement.

Dr. Zhou received the honorary title of "China Electric Power Excellent Young Scientific and Technological Talent," in 2020; and the "Excellent Young Energy Scientist of China," in 2018.

JICHENG YU (Senior Member, IEEE) received the bachelor's degree from the Huazhong University of Science and Technology, Wuhan, China, and the master's and doctoral degrees from Arizona State University, Tempe, USA, all in electrical engineering.

Since 2018, he has been an Engineer and a Scientist with the China Electric Power Research Institute, Wuhan, China. He is dedicated to the research and development of intelligent measurement methods and sensing technologies for power systems. He is the author of three books, more than 40 articles, and more than 60 inventions.

Dr. Yu is a member of IEC TC42 Advisory Group and the Convenor of IEC TC42 WG24.

XIAODONG YIN received the B.S., M.S., and Ph.D. degrees from Wuhan University, all majoring in electrical engineering.

Currently, he is with the Institute of Metrology, China Electric Power Research Institute. He mainly carries out research on frequency voltage proportional standard device and value traceability, metering secondary circuit inspection, and online monitoring of low-voltage current transformers. He has published more than 30 articles and granted more than 50 invention patents in this field.

Dr. Yin was selected as a member of the "Young Talents Support Project" of the Chinese Electrical Engineering Society, in 2017. He received the "Labor Award" of the Chinese Academy of Electrical Engineering, in 2020; the title of "Model Worker" by CEC, in 2020; and the 23rd China Patent Gold Award, in 2022.

CHANGXI YUE received the B.S. and M.S. degrees in electrical engineering from Xi'an Jiaotong University, Xi'an, China, in 2004 and 2006, respectively.

From 2008 to 2011, he was an Engineer with the State Grid Electric Power Research Institute. In 2011, he was with PTB as a Guest Scientist. In 2012, he joined the China Electric Power Research Institute (CEPRI), Wuhan, China, where he currently leads the High-Voltage and High-Current Test Technique Group. He is a senior research engineer experienced in high-voltage and high-current tests and measurements. His research interests include high-voltage and high-current measurement and condition monitoring of the high-voltage equipment.

SIYUAN LIANG received the bachelor's and master's degrees from the University of Electronic Science and Technology of China, in 2017 and 2020, respectively, all in electrical engineering.

Since 2020, he has been an Engineer with the China Electric Power Research Institute, Wuhan, China. He is dedicated to the research and development of intelligent measurement methods and sensing technologies for power systems. He is the author of one book, more than 15 articles, and more than 18 inventions.